

PAPER • OPEN ACCESS

## The effect of geometrical parameters on dimensional deviation in LPBF produced TPMS lattices: a numerical simulation based study

To cite this article: Orhan Gülcan *et al* 2024 *Modelling Simul. Mater. Sci. Eng.* **32** 045009

View the [article online](#) for updates and enhancements.

You may also like

- [Surface curvature in triply-periodic minimal surface architectures as a distinct design parameter in preparing advanced tissue engineering scaffolds](#)  
Sébastien B G Blanquer, Maike Werner, Markus Hannula et al.
- [3D printing polyurethane acrylate\(PUA\) based elastomer and its mechanical behavior](#)  
Huan Li, Lei Liang, Wenxiang Zeng et al.
- [Application of feature fusion strategy for monitoring the condition of nitrogen filled tires using tree family of classifiers](#)  
Hrithik Parihar, S Naveen Venkatesh, P S Anoop et al.

# The effect of geometrical parameters on dimensional deviation in LPBF produced TPMS lattices: a numerical simulation based study

Orhan Gülcan<sup>1</sup> , Kadir Günaydın<sup>1</sup>  and Aykut Tamer<sup>2,\*</sup> 

<sup>1</sup> General Electric Aerospace, Kocaeli, Turkey

<sup>2</sup> University of Bath, Bath, United Kingdom

E-mail: [at2849@bath.ac.uk](mailto:at2849@bath.ac.uk)

Received 20 January 2024; revised 20 March 2024

Accepted for publication 3 April 2024

Published 16 April 2024



CrossMark

## Abstract

Triply periodic minimal surface (TPMS) lattices have drawn great attention both in academic and industrial perspective due to their outstanding mechanical behaviours. Additive manufacturing (AM) modalities enable the production of these lattices very easily. However, dimensional inaccuracy is still one of the problems that AM still faces with. Manufacturing of these lattices with AM modalities, then measuring the critical dimensions and making design changes accordingly is a costly process. Therefore, it is necessary to predict the dimensional deviation of TPMS lattices before print is a key topic. This study focused on prediction of dimensional deviation of laser powder bed fusion (LPBF) produced gyroid, diamond, primitive, IWP and Fisher-Koch lattices by using thermomechanical simulations. TPMS type, unit cell size, volume fraction, functional grading and part orientation were selected as design variables. Results showed that all the design inputs have effects on dimensional accuracy of LPBF produced parts and TPMS type has the most critical factor. Based on analysis of variance analysis, an optimum lattice configuration was proposed to obtain the lowest dimensional deviation after LPBF build.

Keywords: LPBF, TPMS, unit cell size, volume fraction, functional grading, part orientation, process simulation

\* Author to whom any correspondence should be addressed.



Original content from this work may be used under the terms of the [Creative Commons Attribution 4.0 licence](https://creativecommons.org/licenses/by/4.0/). Any further distribution of this work must maintain attribution to the author(s) and the title of the work, journal citation and DOI.

## 1. Introduction

Triply periodic minimal surface (TPMS) lattice structures are one of a kind structures which can be modelled by mathematical expressions and contain unit cells with periodic and regular arrangements [1]. Due to their high energy absorption, specific strength, acoustic and thermal behaviours, these structures are nowadays used in different industrial applications [2]. Different TPMS structures show different mechanical behaviours under axial loading conditions. For instance, primitive structures show stretch-dominated, and gyroid and diamond structures show bending-dominated behaviour under axial loadings [3].

In spite of their outstanding characteristics, the manufacturing of TPMS lattices can be costly and time consuming or sometimes impossible with conventional manufacturing methods, but due to the advancements in different additive manufacturing (AM) modalities, it is now easier to produce these parts from different material alternatives [4]. Laser powder bed fusion (LPBF) is one of the AM processes where metal powders are deposited on a build platform layer by layer and selectively melted by using laser energy. When one layer is melted according to CAD geometry, build platform is lowered with an amount of layer thickness, then new metal powder layer is deposited onto the previous one and this process continues until the part is fully built [5]. LPBF method enables the manufacturing of TPMS lattices however it has some drawbacks one of which is the high dimensional/geometric deviation during manufacturing when compared with the nominal geometry. In LPBF, dimensional/geometric deviation from the CAD model can be occurred due to residual stress and surface roughness which are directly related with process parameters, build orientation, powder inhomogeneities etc [6]. Apart from dimensional deviation, eccentricity differences throughout strut cross section, thickness waviness or in some cases missing walls can be observed [7]. In scientific literature, researchers attributed the dimensional deviation observed in LPBF method to different causes. Davoodi *et al* stated that one of the causes of dimensional deviation in LPBF process is the aggregation of non-fully melted powder particles bonded to overhang surfaces [8]. El Elmi *et al* and Vrana *et al* stated that non fully melted powder particle adhesion, stair step effect or porosities are some of the causes of dimensional variation [9, 10]. Stair step effect was also mentioned in Al-Ketan *et al*'s study [11]. Incomplete melting of metal powders, lack of fusion, entrapped gas porosity can also cause dimensional variations [12]. Bagheri *et al* and other researchers attributed the dimensional deviation in TPMS lattices during LPBF process to different thermal gradients between solid walls/struts and neighbour powders [13–16]. Another cause of dimensional deviation in TPMS lattices during LPBF process is balling phenomena [17, 18]. It is the phenomenon of spreading of metal powders on the build platform especially when high laser velocity or low laser power values are used [19]. Balling phenomena causes mass agglomeration especially at the nodes in lattice structures which results in elliptical shapes of struts during build instead of cylindrical shape [20–22]. Powder particle size difference [23] and data loss during stl export from CAD data [24] were reported as the causes of dimensional deviations.

Dimensional inaccuracies obtained in LPBF method is very important since it directly affects mechanical properties of built part during its service life [25]. Dimensional deviations can be measured after build and related substantiation can be made to effectively use the built part. However, LPBF manufacturing and testing of TPMS lattice structures are costly and time-consuming processes. To eliminate this, thermal and mechanical simulation based finite element modelling, or thermomechanical modelling [26] can be used to predict dimensional deviation before build.

It is observed in the literature that most of the studies focused on compressive properties of TPMS lattices, little attention was given to dimensional deviation prediction [27, 28]. To

address this issue, in the present study, dimensional deviation of five different TPMS lattices produced by LPBF method was predicted by using thermomechanical modelling. TPMS type, volume fraction, unit cell size, functional grading and part orientation were selected as design variables and max. dimensional deviation was selected as the design output. To understand the importance of each variable on design output, analysis of variance (ANOVA) analysis was performed.

The rest of the paper is organized as follows. Lattice geometries, design of experiment, thermomechanical simulation details are explained in section 2. The findings are presented in section 3 and detailed discussions are also given in this section. Section 4 focuses on ANOVA analysis results to understand the effect of each parameter on dimensional deviation and the optimum design parameters to get the min. dimensional deviation. The summary and main conclusions are presented in the Conclusion section.

## 2. Materials and methods

### 2.1. Specimen geometry and design of experiment preparation

MsLattice software [29] was used to prepare TPMS lattice geometries. Gyroid, diamond, primitive, IWP and Fischer-Koch TPMS lattices (figure 1) were used in the present study. These different TPMS types have different surface continuities and different mechanical behaviours under axial loading conditions. Their mathematical expressions are given in equations (1)–(5) below,

$$\text{Gyroid} = \sin(X) \cos(Y) + \sin(Y) \cos(Z) + \sin(Z) \cos(X) \quad (1)$$

$$\text{Diamond} = \cos(X) \cos(Y) \cos(Z) + \sin(X) \sin(Y) \sin(Z) \quad (2)$$

$$\text{Primitive} = \cos(X) + \cos(Y) + \cos(Z) \quad (3)$$

$$\begin{aligned} \text{IWP} = 2 [\cos(X) \cos(Y) + \cos(Y) \cos(Z) + \cos(Z) \cos(X)] \\ - [\cos(2X) + \cos(2Y) + \cos(2Z)] \end{aligned} \quad (4)$$

$$\begin{aligned} \text{Fischer - Koch} = \cos(2X) \sin(Y) \cos(Z) + \cos(X) \cos(2Y) \sin(Z) \\ + \sin(X) \cos(Y) \cos(2Z) \end{aligned} \quad (5)$$

where  $X = 2\pi x/\lambda$ ,  $Y = 2\pi y/\lambda$ , and  $Z = 2\pi z/\lambda$ .  $\lambda$  is the unit cell dimension and  $x$ ,  $y$  and  $z$  are the number of unit cells in related directions [27].

Due to the thin wall manufacturing limitation of LPBF process [30], unit cell size and volume fractions were selected such that the thinnest features have 0.5 mm wall thickness. By considering this limitation, 4, 6 and 8 mm unit cell sizes, 6, 4 and 3 number of unit cells, 25, 35 and 45% volume fractions were selected. All the specimens have outer dimensions of  $24 \times 24 \times 24$  mm. In general, TPMS lattices do not need any support structure during build since they have continuous surfaces with zero mean of curvature. However, in this case, build orientation play an important role on quality of the built part [31]. To understand the effect of build direction on dimensional deviation, the specimens were oriented with four different orientations: 0, 30, 45, 60 degrees (figure 2). To obtain functionally graded specimens, start and end volume fraction values were selected as 25% and 45%, respectively. Therefore, five different functionally graded TPMS lattices with volume fractions changing between 25%–35% were obtained. In total, 57 specimens were modelled and investigated in this study. Table 1 shows the design of experiment consisting of 57 specimens.

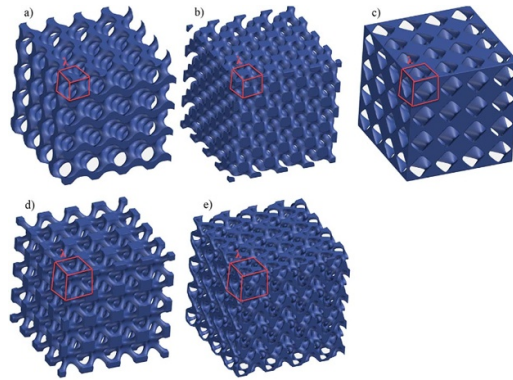


**Figure 1.** The specimens with  $24 \times 24 \times 24$  mm outer dimensions: (a) gyroid, (b) diamond, (c) primitive, (d) IWP, (e) Fischer-Koch.

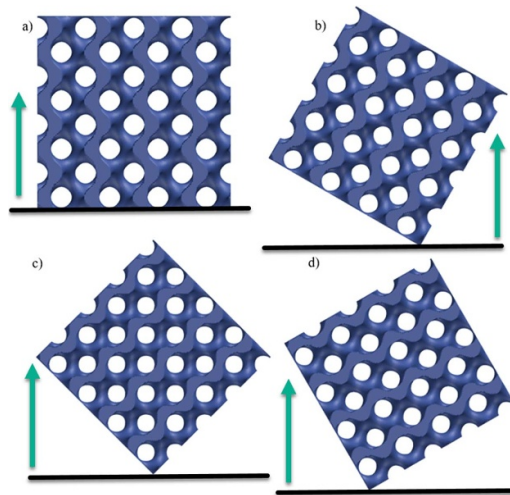


**Figure 2.** Gyroid specimen with four orientations: (a) 0 degree, (b) 30 degree, (c) 45 degree, (d) 60 degree. Black lines represent the upper surface of build platform. Green arrows represent the build direction.

## 2.2. Simulation and mesh convergence study

Thermomechanical simulations were performed in Simufact Additive 4.1 commercial software. To perform back to back comparison, all specimens were simulated by using Inconel 718 alloy powder parameters in Simufact Material library.

Simufact Additive software uses voxel elements to discretize the geometry. The most important selection in thermomechanical simulations is the voxel element size. When lower voxel element sizes are selected, higher accuracy results can be obtained, however, in this case, computation time would be higher. Therefore, in thermomechanical simulations, it is necessary to perform a mesh convergence study by considering accuracy and computation time as design outputs. For this purpose, 0.7, 0.6, 0.5, 0.4, 0.3 and 0.2 mm voxel element sizes were

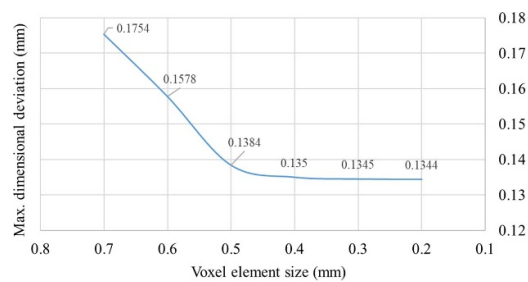
**Table 1.** Design of experiment used in the present study.

Specimen No	Lattice type	Volume fraction	Part orientation (deg)	Unit Cell Size (mm)	Number of unit cell
1	Gyroid	0.25	0	6	4
2	Gyroid	0.25	30	6	4
3	Gyroid	0.25	45	6	4
4	Gyroid	0.25	60	6	4
5	Gyroid	0.35	0	6	4
6	Gyroid	0.35	30	6	4
7	Gyroid	0.35	45	6	4
8	Gyroid	0.35	60	6	4
9	Gyroid	0.45	0	6	4
10	Gyroid	0.45	30	6	4
11	Gyroid	0.45	45	6	4
12	Gyroid	0.45	60	6	4
13	Diamond	0.25	0	6	4
14	Diamond	0.25	30	6	4
15	Diamond	0.25	45	6	4
16	Diamond	0.25	60	6	4
17	Diamond	0.35	0	6	4
18	Diamond	0.35	30	6	4
19	Diamond	0.35	45	6	4
20	Diamond	0.35	60	6	4
21	Diamond	0.45	0	6	4
22	Diamond	0.45	30	6	4
23	Diamond	0.45	45	6	4
24	Diamond	0.45	60	6	4
25	Primitive	0.25	0	6	4
26	Primitive	0.25	30	6	4
27	Primitive	0.25	45	6	4
28	Primitive	0.25	60	6	4
29	Primitive	0.35	0	6	4
30	Primitive	0.35	30	6	4
31	Primitive	0.35	45	6	4
32	Primitive	0.35	60	6	4
33	Primitive	0.45	0	6	4
34	Primitive	0.45	30	6	4
35	Primitive	0.45	45	6	4
36	Primitive	0.45	60	6	4
37	IWP	0.25	0	6	4
38	IWP	0.35	0	6	4
39	IWP	0.45	0	6	4
40	Fisher-Koch	0.25	0	6	4
41	Fisher-Koch	0.35	0	6	4
42	Fisher-Koch	0.45	0	6	4
43	Gyroid	0.25	0	4	6
44	Gyroid	0.25	0	8	3
45	Diamond	0.25	0	4	6
46	Diamond	0.25	0	8	3
47	Primitive	0.25	0	4	6
48	Primitive	0.25	0	8	3

(Continued.)

**Table 1.** (Continued.)

Specimen No	Lattice type	Volume fraction	Part orientation (deg)	Unit Cell Size (mm)	Number of unit cell
49	IWP	0.25	0	4	6
50	IWP	0.25	0	8	3
51	Fisher-Koch	0.25	0	4	6
52	Fisher-Koch	0.25	0	8	3
53	Gyroid	0.25–0.45	0	6	4
54	Diamond	0.25–0.45	0	6	4
55	Primitive	0.25–0.45	0	6	4
56	IWP	0.25–0.45	0	6	4
57	Fisher-Koch	0.25–0.45	0	6	4

**Figure 3.** Mesh convergence study.

used in the thermomechanical simulation of one of the TPMS specimens (gyroid) and dimensional deviations were measured. From figure 3, it is clear that after 0.3 mm voxel element size, the max. dimensional deviation converges to a constant value. Therefore, all the 57 specimens were simulated by using 0.3 mm voxel element size. Figures 4(a) and (b) show CAD geometry of one of the specimens and its discretized version with voxel elements, respectively. The simulation data and CAD data were then aligned in GOM Inspect software and a deviation map was prepared. Max. dimensional deviations were measured on these deviation maps (figure 4(c)).

### 3. Results and discussions

#### 3.1. The effect of TPMS type on dimensional deviation

Max. dimensional deviation results for different TPMS types with fixed volume fraction (0.25), orientation (0 degree), unit cell size (6 mm) and number of unit cells (4) are shown in figure 5. The highest and the lowest dimensional deviations were observed on diamond and Fischer-Koch lattices, respectively. Different TPMS types have different surface continuities, and these surface types and orientations directly affect the thermal distribution in each layer. Different thermal distribution eventually leads different surface qualities in terms of both surface roughness and dimensional deviation [32, 33].

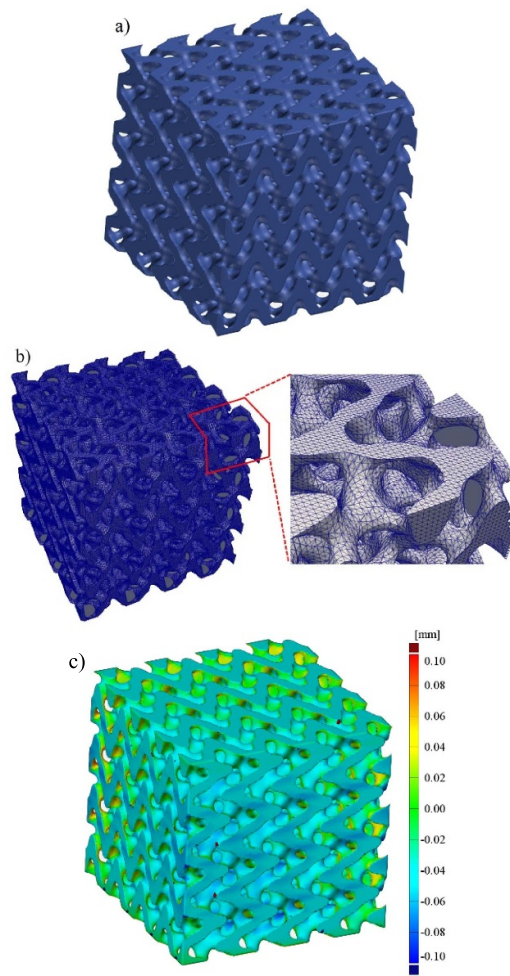


**Figure 4.** (a) Fischer-Koch geometry, (b) discretized geometry with voxel meshes, (c) dimensional deviation map based on superimpose of nominal and simulation geometry.

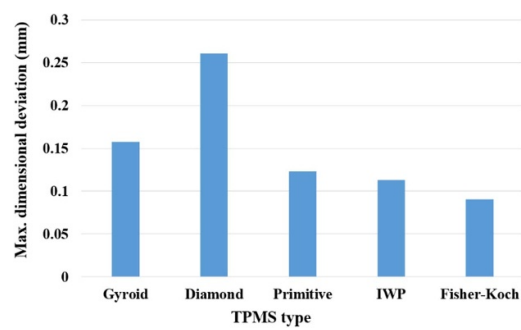


**Figure 5.** The effect of TPMS type on dimensional deviation.

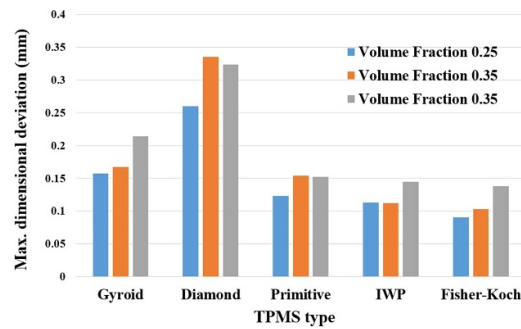


**Figure 6.** The effect of volume fraction on dimensional deviation.

### 3.2. The effect of volume fraction on dimensional deviation

Max. dimensional deviation results for different volume fractions with fixed orientation (0 degree), unit cell size (6 mm) and number of unit cells (4) are shown in figure 6. It is clear that for gyroid, IWP and Fischer-Koch lattices, increase in volume fraction increases the dimensional deviation. On the other hand, for diamond and primitive specimens, dimensional deviation first increases and then decreases when volume fraction increases from 0.25 to 0.35 and then from 0.35 to 0.45, respectively. For the same unit cell size and number of unit cells, increasing the volume fraction of a TPMS lattice results in an increase in wall thickness. Therefore, in each cross sectional area, higher energy input is necessary to melt the related cross section via laser energy which, at the end, causes different thermal deviations between successive layers and finally different dimensional deviations [34]. The effect of volume fraction directly affects compressive behaviours. Higher volume fractions and resulting higher wall thicknesses lead to improved yield and ultimate stress values [35]. The volume fraction directly affects producibility of TPMS lattices for the same reason as well [36].

### 3.3. The effect of unit cell size on dimensional deviation

Max. dimensional deviation results for different unit cell sizes with fixed orientation (0 degree), volume fraction (0.25) and outer dimensions ( $24 \times 24 \times 24$  mm) are shown in figure 7. It can be concluded that for all TPMS types, unit cell size directly influences the dimensional deviation. The higher the unit cell size, the higher the dimensional deviation based on fixed values for other geometrical parameters.

When volume fraction is kept fixed, decreasing unit cell size decreases the TPMS wall thicknesses. To scan lower cross sectional areas, lower scan vectors are used in LPBF method. For this reason, successive scanning becomes quicker and faster. This results in lower time given to the scan line to cool down and in general higher temperatures in lower scanning areas. This high temperature enables fully melting of metal powders. Moreover, thin walls due to lower unit cell sizes cool down more quickly and number of non fully melted powder particle adhesion to these surfaces becomes limited which at the end results in higher dimensional accuracy [37]. This dimensional deviation due to change in unit cell size directly affects mechanical properties as well [38].

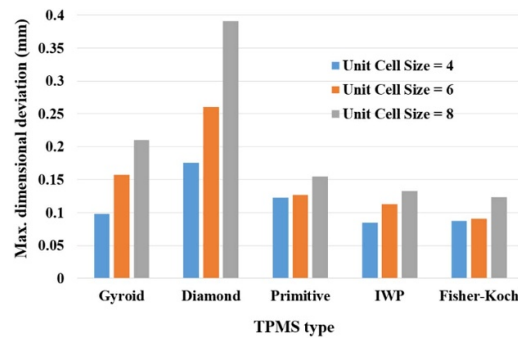


**Figure 7.** The effect of unit cell size on dimensional deviation.

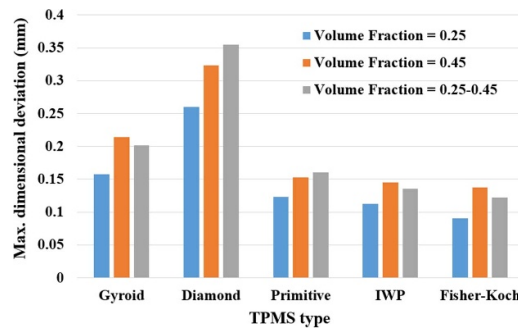


**Figure 8.** The effect of functional grading on dimensional deviation.

### 3.4. The effect of functional grading on dimensional deviation

Max. dimensional deviation results for lattices with 0.25 and 0.45 volume fractions and also with functional grading are shown in figure 8. Unit cell sizes (6 mm) and orientation (0 degree) are fixed for these lattices. For gyroid, IWP and Fischer-Koch lattices, functionally graded specimens showed higher dimensional deviations than the same type of specimens with 0.45 volume fraction. On the other hand, in diamond and primitive lattices, functional grading results in dimensional deviation values between that for specimens with 0.25 and 0.45 volume fractions.

For the fixed volume fractions in TPMS lattices, the scanning area in each layer is similar. However, in functionally graded TPMS lattices, the scanning area, energy input and residual stress formation are different. These result in inhomogeneous thermal gradients and dimensional deviations throughout the specimen. Functional grading in lattice structures have been investigated in literature and different mechanical behaviours were observed when compared with fixed grading lattices [39, 40].

### 3.5. The effect of part orientation on dimensional deviation

The effect of part orientations (0, 30, 45 and 60 degrees) on dimensional deviation results are shown in figure 9 for gyroid, diamond and primitive specimens with different volume fractions. For all TPMS types, it is clear that the highest and the lowest dimensional deviations were observed on specimens with 30 degree and 0 degree orientations, respectively.

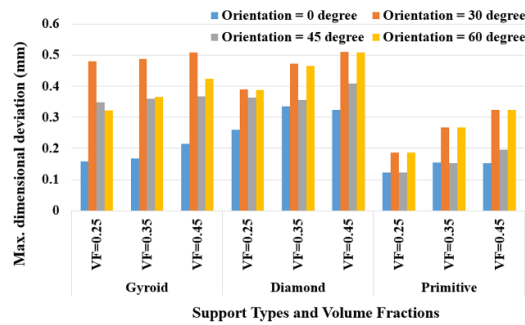


**Figure 9.** The effect of part orientation on dimensional deviation.

For diamond and primitive lattices, dimensional deviation for 30 and 60 degree orientations were nearly the same. It was stated in literature that the orientation of struts/walls in lattice structures with respect to build direction is one of the key elements in surface roughness and dimensional deviations [41]. Orientation of TPMS lattice with respect to build plate or build direction directly affects the orientation of walls/struts which causes different heat transfer phenomena. It was stated in the literature that oriented struts/walls have slower heat transfer due to thermal gradients compared with vertical struts/walls which causes different amount of non-fully melted particle adhesion to the surfaces and different amount of dimensional deviations [42]. In LPBF process, larger melt pools or over-melting occurs on overhang features and this phenomenon becomes more critical when struts or walls in TPMS lattices are more parallel to the build platform which causes more non fully melted particle adhesion to the overhang surfaces [43]. In some scientific studies, up to 100% diameter increase was observed on struts parallel to the build platform [44]. Build orientation does not only effect diameter or thickness but it also affects waviness of walls which results in low quality products [45, 46].

#### 4. ANOVA analysis

To understand the importance of each variable on dimensional deviation, ANOVA analysis was performed in Minitab 20 software. Main effects plot for TPMS type, volume fraction, part orientation and unit cell size in terms of dimensional deviation is shown in figure 10. The optimum parameters to get the minimum dimensional deviation based on existing DOE is Fisher-Koch lattice, functional grading between 0.25–0.45 volume fractions, 0 degree build orientation and 4 mm unit cell size.

Table 2 shows the ANOVA results. In this table, Adj SS (adjusted sum of squares) are measures of variations, Adj MS (adjusted mean squares) means how much variation the related parameter explains, F-value is used to calculate  $p$ -value and  $P$ -value defines significance level which shows the accuracy of the design of experiment [3]. Here, a lower  $P$ -value means higher significance. It is clear that lattice type is the most critical parameter in terms of dimensional deviation. Among four design inputs, it has a contribution of 52.07% on dimensional deviation. On the other hand, unit cell size is the least important factor with a contribution of 0.52% on dimensional deviation.

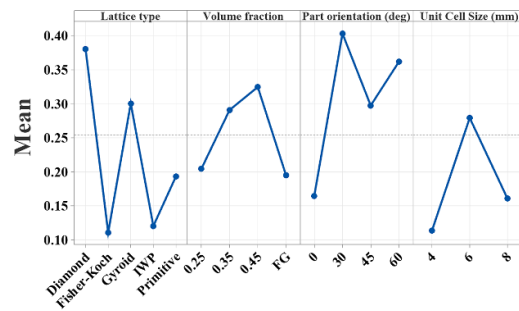


**Figure 10.** Main effects plot for design inputs and outputs. FG means functional grading.

**Table 2.** ANOVA results.

Source	Adj SS	Adj MS	<i>F</i> -Value	<i>P</i> -Value	Contribution
Unit cell size (mm)	0.005 584	0.005 584	1.80	0.186	0.52%
Volume fraction	0.043 582	0.043 582	14.04	0.000	4.08%
Lattice type	0.311 715	0.077 929	25.11	0.000	52.07%
Part orientation (deg)	0.316 884	0.105 628	34.04	0.000	29.67%
Error	0.145 846	0.003 103			13.66%
Total					100.00%

## 5. Conclusions

The prediction of dimensional deviation in different types of TPMS lattices produced by LPBF method is critical in terms of reducing time and cost of iterative trial and error builds. For this purpose, this study focused on prediction of dimensional deviation by using thermomechanical simulations. The effect of TPMS type, volume fraction, unit cell size, functional grading and part orientation on dimensional deviation was investigated both numerically and statistically. The main findings can be listed as below:

- Fischer-Koch lattices outperformed in terms of dimensional deviation. It showed the lowest dimensional deviation. On the other hand, diamond lattices showed the highest dimensional deviation due to different surface continuities.
- Increasing volume fraction by keeping the unit cell size fixed resulted in different behaviour in different TPMS types. This can be attributed to the different energy input needed to fully melt the related scanning area in each layer.
- For all TPMS types, an increase in unit cell size resulted in an increase in dimensional deviation.
- Functional grading leads inhomogeneous scanning areas between successive layers. It was shown that functional grading has a direct influence on dimensional deviation in different ways for different TPMS types.

- Part orientation causes different inclination of TPMS walls. This causes different heat transfer phenomenon between walls and neighbour powders. Therefore, different dimensional deviations were observed for different part orientations.
- Lattice type was found to be the most important parameter in terms of dimensional deviation. An optimum combination of design inputs (Fisher-Koch lattice, functional grading between 0.25–0.45 volume fractions, 0 degree build orientation and 4 mm unit cell size) was proposed to get the lowest dimensional deviation.

This study considered prediction of dimensional deviation in TPMS lattices numerically. Experimental validation is very important to fully show the accuracy of using numerical methods. Therefore, future studies will focus on build and measurement of these lattices and comparison with numerical results.

In the present study, the maximum displacement was taken into account as a measure of numerical simulation prediction accuracy. However, the maximum displacement may be insufficient in some of the industrial applications where a large region with moderate displacements could be observed which is not desired during LPBF process. Future study will take the area of the displacement into account.

### Data availability statement

The data cannot be made publicly available upon publication because they are not available in a format that is sufficiently accessible or reusable by other researchers. The data that support the findings of this study are available upon reasonable request from the authors.

### ORCID iDs

Orhan Gülcan  <https://orcid.org/0000-0002-6688-2662>

Kadir Günaydın  <https://orcid.org/0000-0002-3045-130X>

Aykut Tamer  <https://orcid.org/0000-0003-3257-3105>

### References

- [1] Yin H, Zhang W, Zhu L, Meng F, Liu J and Wen G 2023 *Compos. Struct.* **304** 116397
- [2] Ataollahi S 2023 *Bioprinting* **35** e00304
- [3] Gülcan O, Simsek U, Cokgunlu O, Özdemir M, Şendur P and Yapici G G 2022 *Metals* **12** 1104
- [4] Maconachie T, Leary M, Lozanovski B, Zhang X, Qian M, Faruque O and Brandt M 2019 *Mater. Des.* **183** 108137
- [5] Sefene E M 2022 *J. Manuf. Syst.* **63** 250–74
- [6] Davoodi E *et al* 2022 *Bioact. Mater.* **15** 214–49
- [7] Melancon D, Bagheri Z S, Johnston R B, Liu L, Tanzer M and Pasini D 2017 *Acta Biomater.* **63** 350–68
- [8] Davoodi E *et al* 2021 *ACS Appl. Mater. Interfaces* **13** 22110–23
- [9] El Elmi A, Melancon D, Asgari M, Liu L and Pasini D 2020 *J. Mater. Res.* **35** 1900–12
- [10] Vrana R, Koutny D, Palousek D, Pantelejev L, Jaros J, Zikmund T and Kaiser J 2018 *Materials* **11** 1763
- [11] Al-Ketan O, Rowshan R and Abu Al-Rub R K 2018 *Addit. Manuf.* **19** 167–83
- [12] Sola A and Nouri A 2019 *J. Adv. Manuf. Process.* **1** e10021
- [13] Bagheri Z S, Melancon D, Liu L, Johnston R B and Pasini D 2020 *J. Mech. Behav. Biomed. Mater.* **70** 17–27
- [14] Sing S L, Miao Y, Wiria F E and Yeong W Y 2016 *Biomed. Sci. Eng.* **2** 18–24

- [15] Bartolomeu F, Fonseca J, Peixinho N, Alves N, Gasik M, Silva F S and Miranda G 2019 *J. Mech. Behav. Biomed. Mater.* **99** 1004–117
- [16] Ran Q, Yang W, Hu Y, Shen X, Yu Y, Xiang Y and Cai K 2018 *J. Mech. Behav. Biomed. Mater.* **84** 1–11
- [17] Dallago M, Winiarski B, Zanini F, Carmignato S and Benedetti M 2019 *Int. J. Fatigue* **124** 348–60
- [18] Arabnejad S, Johnston R B, Pura J A, Singh B, Tanzer M and Pasini D 2016 *Acta Biomater.* **30** 345–56
- [19] Dwivedi S, Dixit A R and Das A K 2022 *Mater. Today* **56** 46–50
- [20] Ataei A, Li Y, Fraser D, Song G and Wen C 2018 *Mater. Des.* **137** 345–54
- [21] Lozanovski B, Leary M, Tran P, Shidid D, Qian M, Choong P and Brandt M 2019 *Mater. Des.* **171** 107671
- [22] Alomar Z and Concli F 2020 *Adv. Eng. Mater.* **22** 2000611
- [23] Bartolomeu F, Dourado N, Pereira F, Alves N, Miranda G and Silva F S 2020 *Mater. Sci. Eng. C* **107** 110342
- [24] Calignano F 2018 *Virtual Phys. Prototyp.* **13** 97–104
- [25] Dallago M, Znini F, Carmignato S, Pasini D and Benedetti M 2018 *Proc. Struct. Integr.* **13** 161–7
- [26] Denlinger E R, Gouge M, Irwin J and Michaleris P 2017 *Addit. Manuf.* **16** 73–80
- [27] Álvarez-Trejo A, Cuan-Urquiza E, Bhat D and Roman-Flores A 2023 *Mater. Des.* **233** 112190
- [28] Wu Y, Fang J, Wu C, Li C, Sun G and Li Q 2023 *Int. J. Mech. Sci.* **246** 108102
- [29] Al-Ketan O and Abu Al-Rub R K 2021 *Mater. Des. Process. Commun.* **3** e205
- [30] Simmons C H, Maguire D E and Phelps N 2020 *Manual of Engineering Drawing* 5th edn (Butterworth-Heinemann) pp 585–93
- [31] Alfaify A, Saleh M, Abdullah F M and Al-Ahmari A M 2020 *Sustainability* **12** 7936
- [32] Sokollu B, Gulcan O and Konukseven E I 2022 *Addit. Manuf.* **60** 103199
- [33] Alabort E, Barba D and Reed R C 2019 *Scr. Mater.* **164** 110–4
- [34] Gülcan O, Simsek U, Özdemir M, Günaydın K and Tekoğlu E 2024 *J. Fac. Eng. Archit. Gazi Univ.* **39** 101–12
- [35] Yan C, Hao L, Hussein A, Bubb S L, Young P and Raymont D 2014 *J. Mater. Process. Technol.* **214** 856–64
- [36] Hussein A, Hao L, Yan C, Everson R and Young P 2013 *J. Mater. Process. Technol.* **213** 1019–26
- [37] Yan C, Hao L, Hussein A, Young P, Huang J and Zhu W 2015 *Mater. Sci. Eng.* **628** 238–46
- [38] Du Plessis A, Kouprianoff D P, Yadroitsava I and Yadroitsev I 2018 *Materials* **11** 1663
- [39] Zhang X-Y, Fang G, Leeftang S, Zadpoor A A and Zhou J 2018 *Acta Biomater.* **84** 437–52
- [40] Wu Y C, Kuo C N, Shie M Y, Su Y L, Wei L J, Chen S Y and Huang J C 2018 *Mater. Des.* **158** 256–65
- [41] Liu L, Kamm P, García-Moreno F, Banhart J and Pasini D 2017 *J. Mech. Phys. Solids* **107** 160–84
- [42] Yang E et al 2019 *Mater. Des.* **184** 108165
- [43] Zhang L, Feih S, Daynes S, Chang S, Wang M Y, Wei J and Lu W F 2018 *Addit. Manuf.* **23** 505–15
- [44] Cuadrado A, Yáñez A, Martel O, Deviaene S and Monopoli D 2017 *Mater. Des.* **135** 309–18
- [45] Dong Z, Liu Y, Li W and Liang J 2019 *J. Alloys Compd.* **791** 490–500
- [46] Choy S Y, Sun C, Leong K F and Wei J 2017 *Addit. Manuf.* **16** 213–24